Domain Indexing Collaborative Filtering for Recommender Systems

Rohit Amarnath[1*], Zihao Xu[1*], Qi Xu[2*], Zhigang Hua[2*], Yan Xie[2], Shuang Yang[2], Bo Long[2], Hao Wang[1]

[*]Equal Contribution, [1]Rutgers University, [2]Meta Ranking AI

Reviewed on OpenReview: `https://openreview.net/forum?id=2Wvpq5M42E`

Abstract

In cross-domain recommendation systems, addressing cold-start items remains a significant challenge. Previous methods typically focus on maximizing performance using cross-domain knowledge, often treating the knowledge transfer process as a black box. However, the recent development of domain indexing introduces a new approach to better address such challenges. We have developed an adversarial Bayesian framework, Domain Indexing Collaborative Filtering (DICF), that infers domain indices during cross-domain recommendation. This framework not only significantly improves the recommendation performance but also provides interpretability for cross-domain knowledge transfer. This is verified by our empirical results on both synthetic and real-world datasets.

1 Introduction

In recommender systems, prior user-item interactions are crucial for facilitating accurate recommendations. However, when an item has not previously interacted with any users – known as a "cold-start" item – it becomes challenging to provide high-quality recommendations. This issue is common in cross-domain recommendation, where we train the recommender system on user-item interactions from a source domain but, during inference, encounter items from other domains that the system has never seen before. For example, a recommender system is trained on users and items from the United States, but during inference, it needs to handle items from the United Kingdom.

Extensive efforts have been made to address this problem. For instance, Jiang et al. (2016) proposed a semi-supervised transfer learning approach that uses overlapped-user-based similarities to regularize matrix factorization results. Zhu et al. (2019) introduced special embedding layers to create unique embeddings for users and items in each domain, while the embeddings of overlapping users are a combination of embeddings from different domains. Wang et al. (2015) incorporated additional item and user content information to generate more robust latent representations across domains. While these methods leverage cross-domain information to enhance performance, they often treat the transfer process as a "black box," limiting our understanding and hindering further model improvements. This issue is critical because it can obscure the model's decision-making process, making it difficult to trust and audit.

Recent advances in Domain Adaptation, particularly in domain indexing (Wang et al., 2020a; Liu et al., 2023; Xu et al., 2023; 2022), offer a new perspective on this problem. A domain index – either a scalar or a vector that encodes domain semantics – has been shown to improve model generalization while providing insights into the transfer process (Wang et al., 2020a; Liu et al., 2023; Xu et al., 2023; 2022).

Inspired by this idea, we propose an adversarial Bayesian framework, dubbed *Domain Indexing Collaborative Filtering (DICF)*, which infers domain indices during cross-domain recommendation. The core idea is to aggregate and distill domain-specific features, which then serve as the domain index. This domain index,

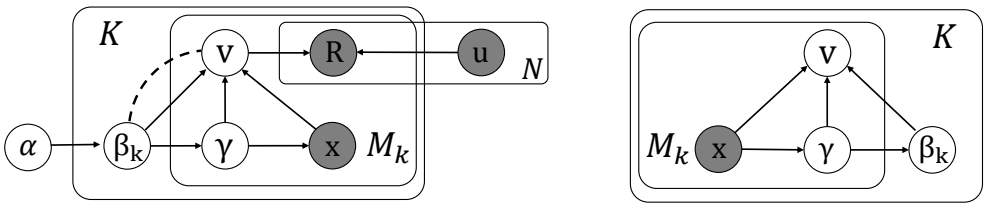

Figure 1: **Left:** Generative model of DICF. The dashed line between β_k and $\mathbf{v}$ indicates that independence is enforced between β_k and $\mathbf{v}$. **Right:** Inference model of DICF. Variables with grey backgrounds represent observed variables; all others are latent.

combined with adversarial learning, enables the model to learn generalizable features, explore domain relationships, and highlight spurious information during cross-domain recommendation, thereby improving our understanding of the process.

Example 1. *(**domain Indices for Recommendation and Interpretability**). Consider the tissue products from Japan, the U.S., and Mexico, which, despite some similarities, vary significantly in descriptions due to language differences. If a recommendation model is trained only using data from Japan and the U.S., it may perform poorly in Mexico due to these linguistic discrepancies. To mitigate this, "unnecessary" or spurious features such as the language of product descriptions across domains should be removed. This resembles standardizing descriptions to English for all domains. A latent variable, termed a domain index, is learned to facilitate this removal. For example, a domain index might be an embedding that denotes the language (e.g., German, Japanese, Spanish) used in product descriptions. This helps indicate how to eliminate domain-index features like the language and preserve generalizable (domain-invariant) features like brand quality and price range. Thus, it effectively serves as a "domain embedding" that captures the essence of the domain. For instance, the domain index for German tissues might be closer to that of Spanish tissues than to Japanese tissues. Such a domain index could improve both the generalization and the interpretability of the model. Further discussion on this will be in Sec. 2.2, "Model Intuition."*

In summary, our contributions are as follows:

- We introduce a novel adversarial Bayesian method, Domain Indexing Collaborative Filtering (DICF), for inferring domain indices in cross-domain recommendation.
- Our experiments on both synthetic and real-world datasets demonstrate that DICF significantly outperforms state-of-the-art methods.
- Visualizations of the domain indices learned by DICF reveal insights into the transfer process, enhancing the interpretability of cross-domain recommendations.

2 Method

In this section, we provide a brief overview of our method, covering the problem setting, model intuition, probabilistic graphical model, and objective function.

2.1 Problem Setting and Notation

In this paper, we address recommendation problems involving a total number of N users and M items, with the items divided into K domains, and each domain k containing M_k items. Each item is characterized by content features represented as an $M \times J$ matrix $\mathbf{x}$, while the user content is given by an $N \times J$ matrix $\mathbf{u}$. The user-item interactions are represented by an $N \times M$ binary matrix R, where a value of "1" indicates that the user likes the item, while "0" indicates either a lack of preference or no interaction with the item. Our model is trained on interactions (ratings) between users and items across K_s source domains, aiming to predict interactions for items in K_t target domains for all users, where $K_s + K_t = K$. Notably, all items in the target domains are cold-start items, meaning that they are not present in the training set.

2.2 Model Intuition

In this subsection, we explain what we mean by the "domain index" in the context of cross-market recommendation, discuss how it facilitates model interpretation and performance, and describe how to derive such a domain index.

In product recommendations, auxiliary data often improves outcomes. For instance, each product typically includes product descriptions and tags – which we refer to as item contexts. Our goal is to learn item representations that generalize effectively from these contexts. Thus, we must eliminate non-generalizable (spurious) features during feature embedding. As illustrated in the introduction, the same item may have contexts in different languages. While product information like brand and price is crucial, the language used should not affect recommendations. Therefore, we separate features into useful and spurious ones, using only the useful for prediction. Spurious features are domain-specific and cannot generalize across domains; thus, they uniquely identify each domain, making them a good source for the domain index.

The *domain index*, aggregated from these spurious features, captures relationships among domains. For instance, we might find that the domain index for U.S. products is closer to that of Mexico than to that of Japan, indicating how the model transfers across different markets. Moreover, since the domain indices embed these domain relationships, we include them as additional inputs to the model, further enhancing performance, as verified in our experiments.

To derive the domain index in an unsupervised manner, we leverage two properties of spurious features: (1) they do not generalize across domains, and (2) they do not facilitate recommendation. Accordingly, we perform this decomposition using adversarial learning. We infer two types of features: the domain index and domain-invariant features. We enforce independence between the domain index and domain-invariant features using a discriminator. We then use only the domain-invariant features for subsequent rating prediction. This ensures that prediction-related information is retained in domain-invariant features, while domain-specific information is captured in the domain index, as proved by Xu et al. (2023). Importantly, our domain index differs from general domain-dependent features: it is a domain-level variable shared by all data points in the same domain, not an instance-level variable. This enables the domain index to uniquely represent each domain.

2.3 Probabilistic Graphical Model of DICF

Based on this intuition, we propose a hierarchical Bayesian deep learning model, Domain Indexing Collaborative Filtering (DICF), to achieve this goal. It follows the generative process illustrated in Fig. 1 (left).

Generative Process of DICF. We assume the generative process below for DICF:

- For each domain k, a domain index $\boldsymbol{\beta}_k$ is generated from a prior distribution $p_\theta(\boldsymbol{\beta}|\boldsymbol{\alpha})$. Here $\boldsymbol{\alpha}$ is the parameter for the prior distribution over the domain index $\boldsymbol{\beta}$.
- Using $\boldsymbol{\beta}_k$, we generate a domain-specific feature $\boldsymbol{\gamma}$ for each item within domain k from $p_\theta(\boldsymbol{\gamma}|\boldsymbol{\beta}_k)$.
- $\boldsymbol{\gamma}$ is then used to generate the item content features $\mathbf{x}$ from $p_\theta(\mathbf{x}|\boldsymbol{\gamma})$, where $\mathbf{x}$ represents the item's observable attributes.
- The item latent vector $\mathbf{v}$ is generated from distribution $p_\theta(\mathbf{v}|\boldsymbol{\beta}_k, \boldsymbol{\gamma}, \mathbf{x})$.
- Finally, the predicted rating $\mathbf{R}$ for each user-item pair is computed using the user vector $\mathbf{u}$ and the item latent vector $\mathbf{v}$ with distribution $p_\theta(\mathbf{R}|\mathbf{u}, \mathbf{v})$. Note that the user vector is generated from the user context using pretrained encoders and is treated as an observed variable.

Inference Process of DICF. In the inference process, we aim to estimate the latent variables $\boldsymbol{\gamma}$, $\boldsymbol{\beta}_k$, and $\mathbf{v}$ from the observed data, as illustrated in Fig. 1 (right). The steps are as follows:

- Given the observed item content features $\mathbf{x}$, we infer the local domain-specific features γ using $q_\phi(\boldsymbol{\gamma}|\mathbf{x})$.
- We aggregate the inferred γ values for all items within domain k to estimate the domain indices $\boldsymbol{\beta}_k$ with distribution $q_\phi(\boldsymbol{\beta}_k|\boldsymbol{\gamma})$, capturing domain-level patterns.
- We infer the item embedding vectors $\mathbf{v}$ based on the estimated $\boldsymbol{\beta}_k$, the content features $\mathbf{x}$, and the local item indices γ with distribution $q_\phi(\mathbf{v}|\boldsymbol{\beta}_k, \boldsymbol{\gamma}, \mathbf{x})$.

Model Factorization. As shown in Fig. 1 (left), we factorize the generative model $p_\theta(\mathbf{x}, \mathbf{u}, \mathbf{v}, \boldsymbol{\beta}, \gamma, \mathbf{R}|\boldsymbol{\alpha})$ into five conditional distributions:

$$p_\theta(\mathbf{x}, \mathbf{u}, \mathbf{v}, \boldsymbol{\beta}, \boldsymbol{\gamma}, \mathbf{R}|\boldsymbol{\alpha}) \tag{1}$$

$$= p_\theta(\mathbf{R}|\mathbf{u}, \mathbf{v}) p_\theta(\mathbf{v}|\mathbf{x}, \boldsymbol{\gamma}, \boldsymbol{\beta}) p_\theta(\mathbf{x}|\boldsymbol{\gamma}) p_\theta(\boldsymbol{\gamma}|\boldsymbol{\beta}) p_\theta(\boldsymbol{\beta}|\alpha). \tag{2}$$

Here, $\boldsymbol{\theta}$ represents the set of parameters for the generative model. We assume that all five distributions follow a Gaussian distribution:

$$p_\theta(\boldsymbol{\beta}|\boldsymbol{\alpha}) = \mathcal{N}(\boldsymbol{\mu}_\alpha, \boldsymbol{\sigma}_\alpha^2), \tag{3}$$

$$p_\theta(\boldsymbol{\gamma}|\boldsymbol{\beta}) = \mathcal{N}(\mu_{\boldsymbol{\gamma}}(\boldsymbol{\beta}; \boldsymbol{\theta}), \sigma_{\boldsymbol{\gamma}}^2(\boldsymbol{\beta}; \boldsymbol{\theta})), \tag{4}$$

$$p_\theta(\mathbf{x}|\boldsymbol{\gamma}) = \mathcal{N}(\mu_x(\boldsymbol{\gamma}; \boldsymbol{\theta}), \sigma_x^2(\boldsymbol{\gamma}; \boldsymbol{\theta})), \tag{5}$$

$$p_\theta(\mathbf{v}|\mathbf{x}, \boldsymbol{\gamma}, \boldsymbol{\beta}) = \mathcal{N}(\mu_v(\mathbf{x}, \boldsymbol{\gamma}, \boldsymbol{\beta}; \boldsymbol{\theta}), \sigma_v^2(\mathbf{x}, \boldsymbol{\gamma}, \boldsymbol{\beta}; \boldsymbol{\theta})), \tag{6}$$

$$p_\theta(\mathbf{R}_{ij}|\mathbf{u}_i, \mathbf{v}_j) = \mathcal{N}(\mathbf{u}_i^T \mathbf{v}_j, \sigma_{\mathbf{R}_{ij}}^2 \mathbf{I}), \tag{7}$$

where in Eqn. 7, $\mathbf{R}_{ij}$ represents the rating given by user i to item j, while $\mathbf{u}_i$ and $\mathbf{v}_j$ denote the feature embeddings for user i and item j, respectively. In our model, $\mathbf{R}_{ij}$ is a binary variable that can take values 0 or 1. We set the variance $\sigma_{\mathbf{R}_{ij}}^2 = \frac{1}{a}$ when $\mathbf{R}_{ij} = 0$ and $\sigma_{\mathbf{R}_{ij}}^2 = \frac{1}{b}$ when $\mathbf{R}_{ij} = 1$. To address the sparsity issue, we choose $a \ll b$. Notice that the use of a Gaussian distribution for R is not intended to model the true generative process of binary feedback. Instead, it serves as a modeling surrogate equivalent to minimizing a weighted squared error, a formulation that is common in the probabilistic matrix factorization literature (Wang et al., 2015).

To approximate the posterior distributions of the latent variables $p_\theta(\mathbf{v}, \boldsymbol{\beta}, \boldsymbol{\gamma}|\mathbf{x})$, we employ an inference distribution $q_\phi(\mathbf{v}, \boldsymbol{\beta}, \boldsymbol{\gamma}|\mathbf{x})$. As illustrated in Fig. 1 (right), we decompose $q_\phi(\mathbf{v}, \boldsymbol{\beta}, \boldsymbol{\gamma}|\mathbf{x})$ as

$$q_\phi(\mathbf{v}, \boldsymbol{\beta}, \boldsymbol{\gamma}|\mathbf{x}) = q_\phi(\boldsymbol{\gamma}|\mathbf{x}) q_\phi(\boldsymbol{\beta}|\boldsymbol{\gamma}) q_\phi(\mathbf{v}|\mathbf{x}, \boldsymbol{\gamma}, \boldsymbol{\beta}), \tag{8}$$

where $\boldsymbol{\phi}$ represents the set of parameters for the inference model. More specifically, we have:

$$q_\phi(\boldsymbol{\gamma}|\mathbf{x}) = \mathcal{N}(\mu_\gamma(\mathbf{x}; \boldsymbol{\phi}), \sigma_\gamma^2(\mathbf{x}; \boldsymbol{\phi})), \tag{9}$$

$$q_\phi(\boldsymbol{\beta}|\boldsymbol{\gamma}) = \mathcal{N}(\mu_\beta(\boldsymbol{\gamma}; \boldsymbol{\phi}), \sigma_\beta^2(\boldsymbol{\gamma}; \boldsymbol{\phi})), \tag{10}$$

$$q_\phi(\mathbf{v}|\mathbf{x}, \boldsymbol{\gamma}, \boldsymbol{\beta}) = \mathcal{N}(\mu_v(\mathbf{x}, \boldsymbol{\gamma}, \boldsymbol{\beta}; \boldsymbol{\phi}), \sigma_v^2(\mathbf{x}, \boldsymbol{\gamma}, \boldsymbol{\beta}; \boldsymbol{\phi})). \tag{11}$$

Note that $\mu_\cdot(\cdot;\cdot)$ and $\sigma_\cdot(\cdot;\cdot)$ denote neural networks; $\boldsymbol{\theta}$, $\boldsymbol{\phi}$ are neural network parameters. The full network structure is illustrated in Fig. 2, where each neural network estimates the density function of each corresponding distribution.

We highlight several key insights for this network structure:

- **Encoder-Decoder Structure for $q_\phi(\boldsymbol{\gamma}|x)$ and $p_\theta(\mathbf{x}|\boldsymbol{\gamma})$.** $p_\theta(\mathbf{x}|\boldsymbol{\gamma})$ aims to reconstruct $\mathbf{x}$ given $\boldsymbol{\gamma}$, encouraging $\boldsymbol{\gamma}$ to preserve as much item context information as possible.
- **Encoder-Decoder Structure for $q_\phi(\boldsymbol{\beta}|\boldsymbol{\gamma})$ and $p_\theta(\boldsymbol{\gamma}|\boldsymbol{\beta})$.** Here, $q_\phi(\boldsymbol{\beta}|\boldsymbol{\gamma})$ aggregates the domain-specific features $\boldsymbol{\gamma}$ to generate the domain index $\boldsymbol{\beta}$. We sample the reconstructed $\hat{\boldsymbol{\gamma}}$ from $p_\theta(\boldsymbol{\gamma}|\boldsymbol{\beta})$ to ensure that $\boldsymbol{\beta}$ captures comprehensive information from $\boldsymbol{\gamma}$.
- **$p_\theta(\mathbf{v}|\mathbf{x}, \boldsymbol{\beta}, \boldsymbol{\gamma})$ regularizes $q_\phi(\mathbf{v}|\mathbf{x}, \boldsymbol{\beta}, \boldsymbol{\gamma})$.** During training, while $q_\phi(\mathbf{v}|\mathbf{x}, \boldsymbol{\beta}, \boldsymbol{\gamma})$ generates the current latent item vector $\mathbf{v}$,
  $p_\theta(\mathbf{v}|\mathbf{x}, \boldsymbol{\beta}, \boldsymbol{\gamma})$ produces another vector $\hat{\mathbf{v}}$ that remains close to the latent vector $\mathbf{v}$ from the previous epoch. This $\hat{\mathbf{v}}$ serves to constrain $\mathbf{v}$, preventing it from deviating significantly from the previous epoch's result, thereby functioning as a regularizer.
- **$p_\theta(\mathbf{R}|\mathbf{u}, \mathbf{v})$ predicts ratings,** similar to the general approach used in matrix factorization.

We follow the approach of Xu et al. (2023) in handling $q_\phi(\boldsymbol{\beta}|\boldsymbol{\gamma})$: First, we aggregate all domain-specific features, $\boldsymbol{\gamma}$, for each domain. Next, we compute a domain distance matrix by measuring the Earth Mover's distance between each set of features. This matrix is then decomposed using multi-dimensional scaling (MDS) to obtain domain embeddings. These embeddings are subsequently fed into a neural network to generate the final domain index.

2.4 Loss Function

Evidence Lower Bound (ELBO). To train the generative and inference models, we employ the evidence lower bound (ELBO) as our objective. By maximizing the ELBO, we can learn the optimal variational distribution $q_\phi(\mathbf{v}, \boldsymbol{\beta}, \mathbf{z}|\mathbf{x})$, which serves as the best approximation to the true posterior distribution of the latent variables $p_\theta(\mathbf{v}, \boldsymbol{\beta}, \boldsymbol{\gamma}|\mathbf{x})$. The ELBO is given by:

$$\mathcal{L}_{ELBO}(\mathbf{x}, \mathbf{u}, \mathbf{R}) = \mathbb{E}_{q_\phi(\mathbf{v}, \boldsymbol{\beta}, \boldsymbol{\gamma}|\mathbf{x})}[\log p_\theta(\mathbf{x}, \mathbf{u}, \mathbf{v}, \boldsymbol{\beta}, \gamma, \mathbf{R}|\boldsymbol{\alpha})] \tag{12}$$

$$- \mathbb{E}_{q_\phi(\mathbf{v}, \boldsymbol{\beta}, \boldsymbol{\gamma}|\mathbf{x})}[\log q_\phi(\mathbf{v}, \boldsymbol{\beta}, \boldsymbol{\gamma}|\mathbf{x})]. \tag{13}$$

With the factorization in Eqn. 2 and Eqn. 8, we decompose the ELBO as (omitting $\boldsymbol{\alpha}$ to avoid clutter):

$$\mathcal{L}_{ELBO}(\mathbf{x}, \mathbf{u}, \mathbf{R}) = \mathbb{E}_{q_\phi(\boldsymbol{\gamma}|\mathbf{x})}[\log p_\theta(\mathbf{x}|\boldsymbol{\gamma})] \tag{14}$$

$$+ \mathbb{E}_{q_\phi(\mathbf{v}, \boldsymbol{\beta}, \boldsymbol{\gamma}|\mathbf{x})}[\log p_\theta(R|\mathbf{u}, \mathbf{v})] \tag{15}$$

$$+ \mathbb{E}_{q_\phi(\boldsymbol{\gamma}|\mathbf{x})}\mathbb{E}_{q_\phi(\boldsymbol{\beta}|\boldsymbol{\gamma})}[\log p_\theta(\boldsymbol{\gamma}|\boldsymbol{\beta})] \tag{16}$$

$$- \mathbb{E}_{q_\phi(\boldsymbol{\gamma}|\mathbf{x})}\big[KL[q_\phi(\beta|\boldsymbol{\gamma})||p_\theta(\boldsymbol{\beta})]\big] \tag{17}$$

$$- KL[q_\phi(\mathbf{v}|\mathbf{x}, \boldsymbol{\gamma}, \boldsymbol{\beta})||p_\theta(\mathbf{v}|\mathbf{x}, \boldsymbol{\gamma}, \boldsymbol{\beta})] \tag{18}$$

$$- \mathbb{E}_{q_\phi(\boldsymbol{\gamma}|\mathbf{x})}[\log q_\phi(\boldsymbol{\gamma}|\mathbf{x})]. \tag{19}$$

Here, Eqn. 14 and Eqn. 16 serve as the reconstruction loss, while Eqn. 15 performs rating regression. Eqn. 17, Eqn. 18 and Eqn. 19 serves as the regularization term. Note that for target domain items, Eqn. 15 is excluded.

Discriminator with an Adversarial Loss. To ensure independence between $\boldsymbol{\beta}$ and $\mathbf{v}$, we introduce an additional discriminator D that is trained using an adversarial loss while simultaneously maximizing the ELBO in Eqn. 13. As demonstrated in Xu et al. (2023), optimizing this adversarial loss to its optimal guarantees that $\boldsymbol{\beta}$ remains independent of $\mathbf{v}$. The discriminator, a neural network $D(\cdot)$, takes $\mathbf{v}$ as input and predicts which domain it comes from, e.g., its domain identity k. In this minimax game, $D(\cdot)$ attempts to classify the domain identity k, while the encoder inference network $q_\phi(\mathbf{v}|\mathbf{x}, \mathbf{u}, \boldsymbol{\beta})$ seeks to produce domain-invariant encodings $\mathbf{v}$ to fool the discriminator. The classification loss for this process is expressed as:

$$\mathcal{L}_{D,\phi} = \mathbb{E}_{p(k,\mathbf{x})}\mathbb{E}_{q_\phi(\mathbf{v}|\mathbf{x})}[\log D(k|\mathbf{v})] \tag{20}$$

Empirical findings generally support the assumption that $\boldsymbol{\beta}$ and $\mathbf{v}$ are independent after training, as discussed in the Sec. 3.6.

Example with Variables a and b. Note that that two random variables a and b can be statistically independent even if a appears as a conditioning variable in the density of b, i.e., $p(b|a)$. Dependence in the *parametrization* of a distribution does not necessarily imply dependence of the resulting random variables.

For example, let $a \sim \mathcal{N}(0, 1)$, define $z = a + 1$, and let $b = z - a$. Then b deterministically equals 1 and is therefore independent of the random variable a, despite being constructed using a.

Connection to $\boldsymbol{\beta}$ and $\mathbf{v}$ in Our DICF. In our model, the domain-invariant item representation $\mathbf{v}$ plays the role of b, the domain index $\boldsymbol{\beta}$ plays the role of a, and the item context $\mathbf{x}$ plays the role of z. Intuitively, the model learns to remove domain-specific information from $\mathbf{x}$ using $\boldsymbol{\beta}$ – conceptually

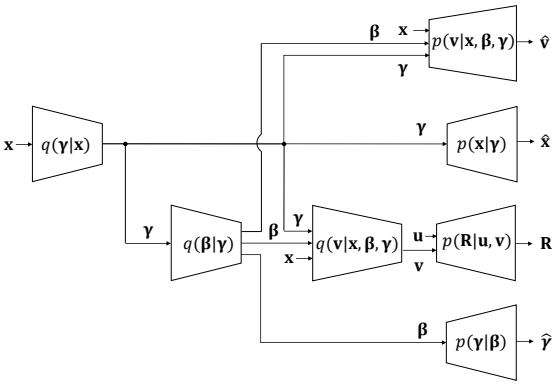

Figure 2: **Network structure.** For simplicity, we omit the subscripts of q_ϕ and p_θ. Intuitively, the functions $q(\boldsymbol{\gamma}|\mathbf{x})$, $q(\boldsymbol{\beta}|\boldsymbol{\gamma})$, $q(\mathbf{v}|\mathbf{x}, \boldsymbol{\beta}, \boldsymbol{\gamma})$ and $p(\mathbf{R}|\mathbf{u}, \mathbf{v})$ generate the instance-level domain-specific feature γ, the domain index β, the item vector $\mathbf{v}$, and the rating $\mathbf{R}$, respectively. Meanwhile, $p(\mathbf{x}|\boldsymbol{\gamma})$, $p(\boldsymbol{\gamma}|\boldsymbol{\beta})$ and $p(\mathbf{v}|\mathbf{x}, \boldsymbol{\beta}, \boldsymbol{\gamma})$ are used to produce reconstructed $\hat{\mathbf{x}}$, $\hat{\boldsymbol{\gamma}}$ and $\hat{\mathbf{v}}$.

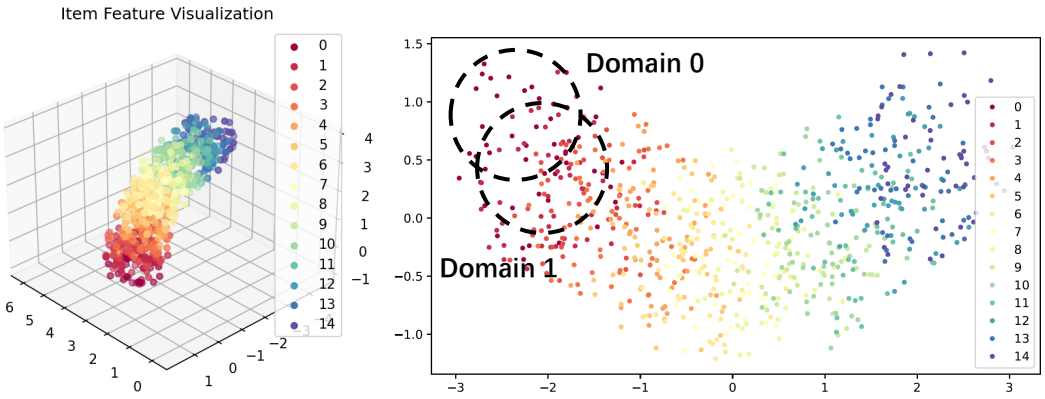

Figure 3: **Left:** Visualization for the item context features $\mathbf{x}$ of Rec-15. The color indicates the domain identities for each item feature. The item feature evolves "gradually" with the domain identity (0, 1, 2, ...). This evolution represents the spurious features intentionally introduced in Rec-15. **Right:** A PCA transformation of the raw item features into two dimensions, with circles denoting the first two domains. The colors indicate different domain identities associated with each item feature.

similar to a "subtraction" $(z - a)$ of domain effects – so that the resulting representation $\mathbf{v}$ is domain-invariant. Although $\boldsymbol{\beta}$ is used as an input to the network, the **adversarial loss** ensures that the learned $\mathbf{v}$ contains no information about $\boldsymbol{\beta}$ and is therefore independent of it in distribution.

Final Objective Function. Our final objective function can be derived by combining Eqn. 13 and Eqn. 20:

$$\begin{aligned}\max_{\theta,\phi}\min_{D}\ \mathcal{L}_{DICF} &= \max_{\theta,\phi}\min_{D}\ \mathcal{L}_{\theta,\phi} - \lambda_d \mathcal{L}_{D,\phi} \\ &= \max_{\theta,\phi}\min_{D}\ \mathbb{E}_{p(\mathbf{x},\mathbf{u},\mathbf{R})}[\mathcal{L}_{ELBO}(\mathbf{x},\mathbf{u},\mathbf{R})] \qquad (21) \\ &\quad - \lambda_d \mathbb{E}_{p(k,\mathbf{x})}\mathbb{E}_{q_\phi(\mathbf{v}|\mathbf{x})}[\log D(k|\mathbf{v})], \qquad (22)\end{aligned}$$

with $\mathcal{L}_{\theta,\phi} = \mathbb{E}_{p(\mathbf{x},\mathbf{u},\mathbf{R})}[\mathcal{L}_{ELBO}(\mathbf{x},\mathbf{u},\mathbf{R})]$ and λ_d serving as a balancing hyper-parameter.

Remark: ELBO and the Adversarial Loss. Note that in the final objective function above:

- **ELBO in Eqn. 21.** Specifically, maximizing the ELBO $\mathcal{L}_{ELBO}(\mathbf{x},\mathbf{u},\mathbf{R})$ in Eqn. 21 effectively trains the neural network parameters ϕ to approach the marginal likelihood of the observed data (R, x, u) under our model. Consequently, this process minimizes the KL divergence between (1) the variational approximation (our model) of the posterior distributions over γ, β, and v, i.e., $q_\phi(\gamma \mid x)$, $q_\phi(\beta \mid \gamma)$, and $q_\phi(v \mid x, \gamma, \beta)$ and (2) their true posterior distributions.
- **Adversarial Loss in Eqn. 22.** Eqn. 22 introduces an additional adversarial training loss designed to enhance the model's generalization and interpretability. Importantly, this component complements rather than interferes with the objective in Eqn. 21.

3 Experiments

In this section, we demonstrate our method's effectiveness in generalization and interpretability.

3.1 Datasets

We evaluate our model on 4 datasets, Rec-15, Rec-30, XMRec (Bonab et al., 2021), and MovieLens (Harper & Konstan, 2015).

Rec-15. We created a synthetic recommendation dataset called Rec-15, consisting of 750 users and 750 items. The items are divided into 15 domains, with each domain containing 50 items.

Table 1: Recall@300 (%) and F1-score@300 (%) on *Rec-15* and *Rec-30*. We highlight the best result with **bold face** and the second-best results with underline.

Dataset		PMF	CDL	DANN	MDD	TSDA	DICF (Ours)
Rec-15	Recall	82.3	63.1	83.2	61.3	77.1	**99.2**
	F1-score	7.2	**25.5**	7.5	6.9	7.0	10.0
Rec-30	Recall	21.1	20.7	28.4	26.8	19.0	**66.0**
	F1-score	17.9	18.1	20.9	20.2	29.8	**40.0**

The intuition is that we add linearly increasing spurious features to the "true item feature". We intend for our model to infer the domain index's linear growth and learn adaptive item latent vectors across different domains. We detail below the generation processes of user features $\mathbf{u}$, item contexts $\mathbf{x}$, and ground truth ratings R.

For each user, we generate a 2-dimensional unit vector $[a, b]$ at random. The user feature vector $\mathbf{u}$ is then defined as $\mathbf{u} = [r + a, b]$, where r is a constant offset typically set to 2.

For each item domain k (where $k = 0, 1, \ldots, 14$), we compute an angle $\theta = \frac{k\pi}{30}$ and define the domain cluster center as $\boldsymbol{\mu} = [r,\ r(\cos\theta - 1),\ r\sin\theta]$. We then sample a 3-dimensional item context feature $\mathbf{x} = [c_1, c_2, c_3]$ from the normal distribution $\mathcal{N}(\boldsymbol{\mu}, \mathbf{I})$, where $\mathbf{I}$ is a 3-dimensional identity vector. Fig. 3 shows the generated item features.

The ground truth rating R is generated as the dot product of the user feature $\mathbf{u} = [r + a, b]$ and the "true item feature" given by $\mathbf{v} = [c_1,\ \sqrt{(r + c_2)^2 + c_3^2} - r]$.

For training, we select items from domains 0 to 4 and use items from the remaining domains as testing data.

Rec-30. We also created another synthetic dataset called Rec-30 using the same procedure as Rec-15, except that it contains 30 item domains, with a total of 1,500 users and 1,500 items. Again, we select items from domains 0 to 5 for training and use the others for testing.

Table 2: Recall@300 (%) and F1-score@300 (%) for XMRec on *Souce-Rich* and *Souce-Poor* tasks across different target markets. We highlight the best result with **bold face** and the second-best results with underline.

Task	Target Market	PMF		CDL		DANN		MDD		TSDA		DICF (Ours)	
		Recall	F1-score	Recall	F1-score	Recall	F1-score	Recall	F1-score	Recall	F1-score	Recall	F1-score
Source-Rich	Canada	18.6	1.5	18.9	1.5	19.9	1.6	17.2	1.4	26.5	2.1	**37.2**	**3.0**
	France	65.6	5.3	62.0	5.0	68.2	5.4	65.8	5.2	66.1	5.3	**73.0**	**5.7**
	India	9.9	0.9	14.5	1.2	11.4	0.1	9.6	0.8	10.0	0.9	**20.6**	**1.8**
	Spain	28.2	2.4	28.4	2.4	29.3	2.4	28.4	0.3	36.6	3.1	**40.0**	**3.4**
	UK	13.4	1.1	13.6	1.1	11.9	0.1	12.4	1.0	11.5	0.9	**24.3**	**2.0**
	Average	27.1	2.2	27.5	2.2	28.1	1.9	26.8	1.7	30.1	2.5	**39.0**	**3.2**
Source-Poor	Germany	3.8	0.3	5.8	0.5	3.8	0.3	4.2	0.4	3.4	0.3	**8.7**	**0.8**
	Italy	20.5	1.8	24.5	2.1	22.7	1.9	18.4	1.6	15.0	1.3	**38.2**	**3.2**
	Japan	18.4	1.5	18.9	1.5	20.5	1.7	19.3	1.6	16.4	1.3	**37.2**	**3.0**
	Mexico	9.1	0.8	14.4	1.2	11.2	1.0	10.5	0.9	8.2	0.7	**20.6**	**1.8**
	US	1.1	0.1	2.0	**0.2**	1.1	0.1	1.0	0.1	1.0	0.1	**2.1**	**0.2**
	Average	10.6	0.9	13.1	1.1	11.9	1.0	10.7	0.9	8.8	0.7	**18.8**	**1.8**

XMRec (Bonab et al., 2021). The XMRec dataset is a cross-market recommendation dataset that encompasses 18 local markets and 16 distinct product categories, and 52.5 million user-item interactions. We utilize item descriptions from this dataset to generate item context features with the help of Sentence-BERT (Reimers & Gurevych, 2020), and subsequently create user features based on the first three items they purchased. Users with fewer than ten purchases are excluded from our experiments. To simplify the analysis, we also remove items and users that appear in multiple countries. Additionally, we exclude market data from

Table 3: Recall@300 (%) and F1-score@300 (%) for MovieLens. We highlight the best result with **bold face** and the second-best results with underline.

Target Movie Years	PMF		DANN		CDL		TSDA		MDD		DICF (Ours)	
	Recall	F1-score	Recall	F1-score	Recall	F1-score	Recall	F1-score	Recall	F1-score	Recall	F1-score
1971-1980	57.46	7.66	65.31	8.55	60.28	8.12	37.35	8.36	**68.34**	**8.98**	61.36	8.03
1986-1990	41.64	6.33	47.67	7.12	42.78	6.47	45.65	6.44	28.58	4.55	**48.77**	**7.16**
1991-1993	48.90	6.13	45.61	5.96	49.60	6.13	44.31	6.13	43.44	5.84	**57.70**	**7.03**
1994-1997	14.64	3.17	14.70	3.26	14.58	3.17	**32.40**	**4.55**	13.24	3.06	18.90	3.90
1998-2000	25.65	4.64	24.53	4.50	25.58	4.66	**33.88**	4.33	23.31	4.10	33.31	**5.71**
Average	37.66	5.59	37.14	5.88	37.43	5.71	38.72	5.94	34.52	5.31	**44.01**	**6.37**

Singapore, China, and Australia due to insufficient numbers of items and users. After this filtering process, our experiments are conducted with 14,412 users and 48,721 items across 10 countries.

Here we focus on two tasks for XMRec:

- **Source-Rich**: Train models in data-rich source markets (Germany, Italy, Japan, Mexico, and US) and test in data-poor target markets (Canada, France, India, Spain, and UK).
- **Source-Poor**: Train models in data-poor source markets (Canada, France, India, Spain, and UK) and test in data-rich target markets (Germany, Italy, Japan, Mexico, and US).

MovieLens (Harper & Konstan, 2015). MovieLens is a movie rating dataset including films from 1920 to 2000. We use the OMDB API (Fritz, 2023) to retrieve contextual information (mainly the plot and title) and employ MiniLM (Wang et al., 2020b) to generate item features. The movies are divided into 11 categories by production year (e.g., 1941 to 1950). We use movies from 1919-1970 and 1981-1985 as source domains, and those from 1971-1980 and 1986-2000 as target domains. Following methods similar to XMRec, user features are derived from the first three movies each user rated. Users who have rated fewer than five movies or have no movie rated above 3 are excluded. After such filtering, all experiments are conducted with 6,034 users and 3,705 items.

3.2 Evaluation Metrics

We employ two metrics for evaluation: recall@M and F1-score@M. For each user i, we first rank all the held-out items based on the predicted ratings. Let $J_{i,r}$ represent the r-th ranked item for user i, S_i denote the set of "liked" items for user i, and T be the total number of items ($T \geq M$). The recall@M for user i is defined as follows:

$$\text{recall@M}(i) = \frac{\sum_{r=1}^{M} 1^{J_{i,r} \in S_i}}{|S_i|} \tag{23}$$

Next, we define the precision@M and F1-score@M for user i as follows:

$$\text{precision@M}(i) = \frac{\sum_{r=1}^{M} 1^{J_{i,r} \in S_i}}{M} \tag{24}$$

$$\text{F1-score@M}(i) = \frac{2 \times \text{recall@M}(i) \times \text{precision@M}(i)}{\text{recall@M}(i) + \text{precision@M}(i)} \tag{25}$$

The final result is reported as the average for all users for both metrics.

3.3 Baselines

We compare our proposed method with both the state of arts methods from both domain adaptation and cross-domain matrix factorization, including Probabilistic Matrix Factorization (**PMF**) (Mnih & Salakhutdinov, 2007), Collaborative Deep Learning (**CDL**) (Wang et al., 2015) Domain Adversarial Neural Networks

(**DANN**) (Ganin et al., 2016), Margin Disparity Discrepancy (**MDD**) (Zhang et al., 2019b), and Taxonomy-Structured Domain Adaptation (**TSDA**) (Liu et al., 2023). Note that CDL (Wang et al., 2015) can be viewed as a special case of our model without domain indexing, and therefore serves as a natural ablation baseline. For all the domain adaptation baselines, we use the user feature as an extra input and do feature alignment on the item feature.

3.4 Implementation Details

Rec-15 and Rec-30. For both datasets, we used a domain index dimension of 2. Both models were trained using the Adam optimizer, with learning rates linearly decaying from 7.88×10^{-5} to 1×10^{-8}. For the discriminator, we used $\lambda_d = 0.32$ for Rec-15 and $\lambda_d = 5.3$ for Rec-30. A batch size of 16 was used for both models.

XMRec and MovieLens. For the source-poor task of XMRec, we used a domain index dimension of 2, and for the other tasks, we used a dimension of 5. All models were trained using the Adam optimizer with learning rates linearly decaying from 7.88×10^{-5} to 1×10^{-8}. For the discriminator, we used $\lambda_d = 0.7$ for the source-rich task and $\lambda_d = 0.8$ for the source-poor task. A batch size of 32 was used for both models.

Baseline Implementation. For all baseline methods as well as our own, we set the latent size of both user and item latent vectors to 512. For PMF, we used a learning rate of 0.01, a batch size of 32, and conducted training over 100 epochs. In the case of the DANN model, the grid search indicated that incorporating an early stopping strategy enhances performance, setting the learning rate at 0.01, batch size at 32, and limiting training to 10 epochs across different datasets. For CDL, we adjusted the learning rate to 0.001, increased the batch size to 128, and extended training to 600 epochs, accounting for the lower learning rate. TSDA and MDD models were configured using the default hyperparameters.

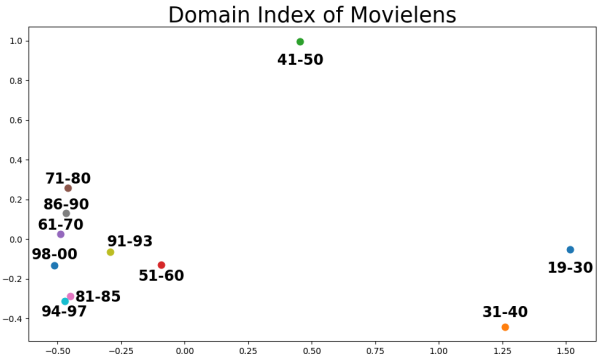

Figure 4: Inferred domain indices (reduced to 2 dimensions by PCA) for MovieLens. Numbers near the domain indices show each domain's movie year range. We only use the last two digits for simplicity – for example, "98–00" stands for "1998–2000". Note that DICF does not have access to these ground truth indices during training.

3.5 Results

Rec-15 & Rec-30. Table 1 show the results for the Rec-15 and Rec-30 datasets under different metrics. Though CDL outperforms DICF on the F1-score of Rec-15, DICF still holds a substantial lead over other models. Specifically, it achieves an F1-score@300 of 40.0% and a Recall@300 of 66.0%, far ahead of the all the other models by over a 10 % margin. These results demonstrate DICF's effectiveness in identifying relevant items (high recall) and in delivering precise recommendations (high F1-score). The performance difference between Rec-15 and Rec-30 indicates that as the number of domains increases, our model tends to perform better, since additional domains provide richer training signals for domain indexing.

XMRec. Table 2 shows the results for XMRec under different metrics. In the Source-Rich scenario, DICF outperforms competitors on both F1-score and Recall. For instance, in Italy DICF achieves an F1-score of 3.0% and a Recall of 37.2%. This trend is consistent across other countries in the source-rich scenario, helping DICF achieve the highest average score across these markets. In the Source-Poor setting, DICF also leads. It reaches an F1-score of 1.8 %, which is 63.6 % higher than the next-best model, CDL (1.1 %), and a Recall of 18.8 %, over 5 percentage points higher than CDL.

MovieLens. Table 3 shows the MovieLens results. DICF outperforms all other models on movies from 1986–1990 and 1991–1993 by a large margin, achieving improvements of at least 3.6% in the average recall and F1-score of all domains.

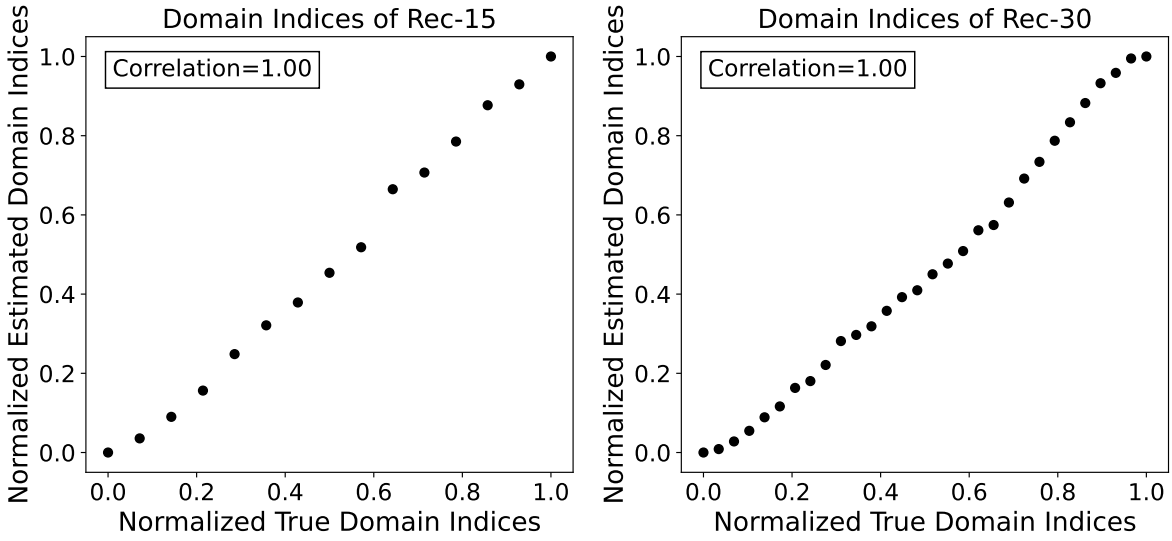

Figure 5: Normalized domain indices (reduced to 1 dimension by PCA) for 15 domains in *Rec-15* (**left**) and 30 domains in *Rec-30* (**right**). DICF successfully inferred linear domain indices, demonstrating a high correlation with the ground truth domain indices. Note that DICF does not have access to these ground truth indices during training.

Visualizing Domain Indices. We also visualize the domain indices obtained from different datasets using Principal Component Analysis (PCA).

For Rec-15 and Rec-30, as illustrated in Fig. 5, the domain indices align along a linear trajectory when plotted against the ground truth domain indices. Note that during data generation, we explicitly adding linearly growing spurious features to the "true" feature. This visualization result, combined with the numerical results presented in Table 1 , highlights that our model successfully infers non-trivial domain indices and produces item latent vectors capable of generalizing across different domains.

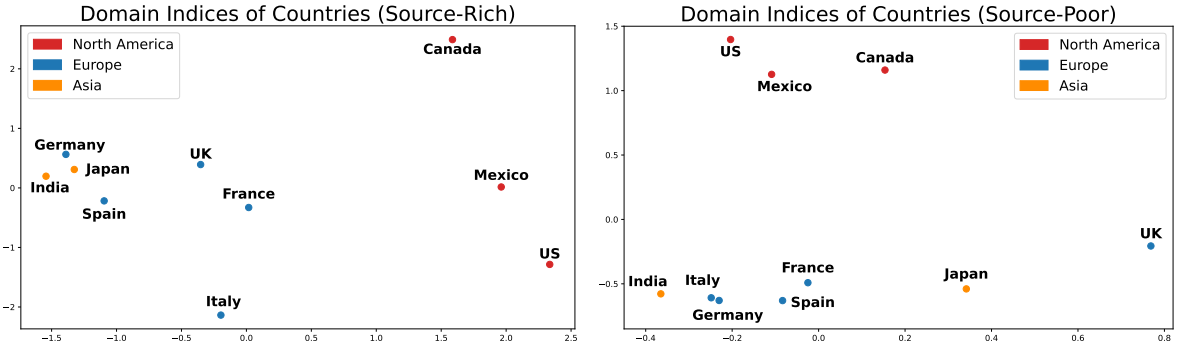

Figure 6: Inferred domain indices (reduced to 2 dimensions by PCA) for XMRec in *Source-Rich* setting (**left**) and *Source-Poor* setting (**right**). Countries are colored according to their continents. We emphasize that the model did not receive any continental/geographic information during training.

In Fig. 4, the MovieLens domain indices naturally forms clusters according to movie release years. Indices for movies from 19–30, 31–40, and 41–50 group together, while those for 81–85, 91–93, 94–97, and 98–00 form another cluster. Similar patterns appear for other domain indices, indicating that DICF recognizes closer relationships among domains with similar movie release years. This demonstrates that our model can learn non-trivial relationships between domains.

For XMRec, we observe a correlation between the domain indices and the geographical/continental information of the countries in Fig. 6. For instance, in Fig. 6 (left) under the Source-Rich setting, domain indices of countries within the same continent are closer, such as the US being closer to Mexico than to India. Additionally, within the same continent, the domain index distances reflect geographical proximity, e.g., the UK is closer to France than to Spain and Italy.

Note that Japan's domain index is positioned close to Western countries while remaining relatively isolated, i.e., it is close to both European countries like Germany and Asian countries like India. One possible interpretation is that, although Japan is an Asian country, it has been strongly influenced by Western culture, institutions, and economic systems. This influence may explain its proximity to Western domains, while its distinct historical, cultural, and social characteristics contribute to its relative isolation. This nuanced positioning highlights an interesting phenomenon that merits further investigation, which we leave for future work.

Under the Source-Poor setting (Fig. 6 (right)), despite some degradation in the quality of domain indices, there is still a clear clustering of European and North American countries.

Based on the analysis in Sec. 2.2, we can conclude that: **1)** During knowledge transfer, the model recognizes a closer relationship among items from countries within the same continent or with closer geographical distances. **2)** It identifies geographical/continental information as a spurious feature to be removed. By eliminating the geographical/continental information from the item features, we derive a more generalizable representation suitable for cold-start item recommendations.

In summary, it is clear that our DICF framework significantly advances our understanding of the knowledge transfer process, thereby enhancing the model's interpretability.

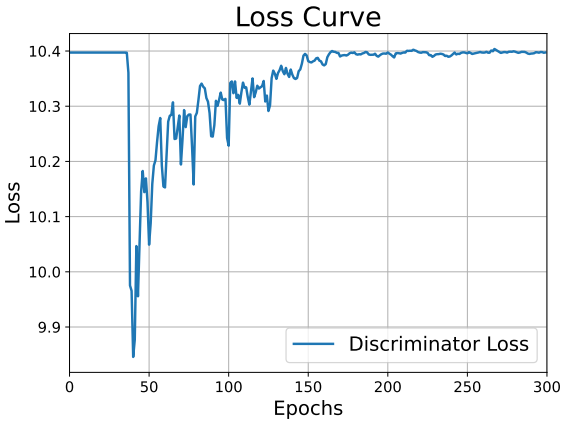

Figure 7: Visualization for discriminator loss during training. The loss initially decreases and then returns to its initial value, indicating that D returns to random classification again. This means the inferred domain indices are independent of domain-invariant features after the training.

3.6 Discussion

Independence of Domain Indices and Domain Invariant Features. Our method assumes that domain indices are independent of domain-invariant features after training. Such independence assumption is generally supported by the stable pattern of discriminator D's loss. Typically, D starts by randomly classifying domains. Although the loss decreases early in the training, it eventually returns to its initial value (Fig. 7), suggesting D reverts to random classification due to the domain-invariant features. Xu et al., 2023 proves that if features are domain-invariant, the domain index should be independent of these features. Consistent replication of this result across various experiments and hyperparameters solidifies our confidence in this independence assumption.

The Role of the Adversarial Loss. We have conducted an ablation study on the adversarial loss (similar to a GAN loss) using the Rec-30 dataset. In Table 4, we can see that when the GAN loss is removed, the model performance degrades substantially on Precision and F1-score, while Recall almost remains unchanged.

This indicates that the adversarial loss plays a crucial role in **improving the quality of the learned item representations rather than merely increasing coverage**. Without the adversarial constraint, domain-specific infor-

Table 4: Ablation study on the effect of adversarial loss (similar to a GAN loss).

Model Variant	Prec@ 300 (%)	Rec@ 300 (%)	F1@ 300 (%)
DICF	28.7	66.0	40.0
DICF w/o GAN loss	16.0	66.0	25.7

mation leaks into the item latent vector, leading to lower
ranking precision even though the model can still retrieve a similar number of relevant items.

By enforcing domain invariance through adversarial training, the GAN loss ensures that only preference-relevant, domain-invariant features are retained in the item representations; it removes domain-specific features that do **not** generalize across different domains. As a result, it can significantly improve ranking accuracy and overall recommendation quality across domains.

4 Related Works

Domain Adaptation. Domain adaptation has been extensively studied (Pan & Yang, 2009; Pan et al., 2010; Ganin et al., 2016; Long et al., 2018; Saito et al., 2018; Sankaranarayanan et al., 2018; Zhang et al., 2019b; Peng et al., 2019; Chen et al., 2019; Dai et al., 2019; Nguyen-Meidine et al., 2021; Zou et al., 2018; Kumar et al., 2020; Prabhu et al., 2021; Farahani et al., 2021; Mancini et al., 2019; Tasar et al., 2020; Jin et al., 2022) to leverage prior knowledge to improve the performance of models in new environments. Various approaches have been developed for domain adaptation, with adversarial learning (Ganin et al., 2016; Ben-David et al., 2010; Tzeng et al., 2017; Zhang et al., 2019b; Kuroki et al., 2019; Chen et al., 2019; Dai et al., 2019) emerging as one of the most effective due to its high performance. Typically, adversarial learning focuses on learning domain-invariant features that generalizes across domains. Recently, several studies (Wang et al., 2020a; Xu et al., 2022; Liu et al., 2023; Xu et al., 2023) have introduced domain indices alongside adversarial learning to further improve model generalization and interpretability. Building on this intuition, our work directly extend the ideas of (Xu et al., 2023) to the field of cross-domain recommendation.

Cross-Domain Recommendation. Cross-domain recommendation (Khan et al., 2017; Zhu et al., 2021a; Zang et al., 2022) focuses on utilizing information from different domains to address issues like cold-start and data sparsity. Scenarios typically differ based on whether there is overlap in users or items across domains. Our research specifically targets scenarios where there is no overlap in items and only partial overlap in users. Common approaches to these challenges include Collective Matrix Factorization (Jiang et al., 2016; Rafailidis & Crestani, 2017; Yang et al., 2017; Zhang et al., 2018; Zhu & Chen, 2022), Representation Combination for Overlapping Users (Perera & Zimmermann, 2017; Zhu et al., 2019; 2020; 2021b), and Embedding Mapping (Man et al., 2017; Wang et al., 2018; Fu et al., 2019; Li & Tuzhilin, 2021; Nahta et al., 2025). However, most of the works do not address our zero-shot problem setting, which lacks user-item interactions in the target item domains. Some methods require initial interactions (Zhang et al., 2019a; Zhu & Chen, 2022; Nahta et al., 2025), while others require additional contexts such as knowledge graphs (Bi et al., 2020; Lu et al., 2024) for making recommendations. In addition, no prior work has explicitly extracted domain indices using adversarial learning to enhance both the performance and interpretability of the model.

5 Conclusions

In this paper, we addressed the challenge of cold-start items in cross-domain recommendation systems by introducing the Domain Indexing Collaborative Filtering (DICF) framework. This adversarial Bayesian approach infers domain indices during the recommendation process, significantly improving performance and providing interpretability for cross-domain knowledge transfer. Future research could extend our framework to accommodate dynamic domains where user preferences and domain characteristics evolve over time. We believe that our DICF framework opens new avenues for both improving recommendation systems and advancing the interpretability of cross-domain knowledge transfer.

Acknowledgement

We thank all reviewers and AE for their valuable comments. HW is supported by Amazon Faculty Research Award, Microsoft AI & Society Fellowship, NSF CAREER Award IIS-2340125, NIH grant R01CA297832, and NSF grant IIS-2127918.

References

Shai Ben-David, John Blitzer, Koby Crammer, Alex Kulesza, Fernando Pereira, and Jennifer Wortman Vaughan. A theory of learning from different domains. *Machine learning*, 79(1):151–175, 2010.

Ye Bi, Liqiang Song, Mengqiu Yao, Zhenyu Wu, Jianming Wang, and Jing Xiao. Dcdir: A deep cross-domain recommendation system for cold start users in insurance domain. In *Proceedings of the 43rd international ACM SIGIR conference on research and development in information retrieval*, pp. 1661–1664, 2020.

Hamed Bonab, Mohammad Aliannejadi, Ali Vardasbi, Evangelos Kanoulas, and James Allan. Cross-market product recommendation. In *Proceedings of the 30th ACM International Conference on Information & Knowledge Management*, pp. 110–119, 2021.

Ziliang Chen, Jingyu Zhuang, Xiaodan Liang, and Liang Lin. Blending-target domain adaptation by adversarial meta-adaptation networks. In *Proceedings of the IEEE/CVF Conference on Computer Vision and Pattern Recognition*, pp. 2248–2257, 2019.

Shuyang Dai, Kihyuk Sohn, Yi-Hsuan Tsai, Lawrence Carin, and Manmohan Chandraker. Adaptation across extreme variations using unlabeled domain bridges. *arXiv preprint arXiv:1906.02238*, 2019.

Abolfazl Farahani, Sahar Voghoei, Khaled Rasheed, and Hamid R Arabnia. A brief review of domain adaptation. *Advances in data science and information engineering: proceedings from ICDATA 2020 and IKE 2020*, pp. 877–894, 2021.

Brian Fritz. Omdb api, 2023. URL `https://www.omdbapi.com/`.

Wenjing Fu, Zhaohui Peng, Senzhang Wang, Yang Xu, and Jin Li. Deeply fusing reviews and contents for cold start users in cross-domain recommendation systems. In *Proceedings of the AAAI Conference on Artificial Intelligence*, volume 33, pp. 94–101, 2019.

Yaroslav Ganin, Evgeniya Ustinova, Hana Ajakan, Pascal Germain, Hugo Larochelle, Fran**c**cois Laviolette, Mario Marchand, and Victor Lempitsky. Domain-adversarial training of neural networks. *JMLR*, 17(1): 2096–2030, 2016.

F Maxwell Harper and Joseph A Konstan. The movielens datasets: History and context. *Acm transactions on interactive intelligent systems (tiis)*, 5(4):1–19, 2015.

Meng Jiang, Peng Cui, Nicholas Jing Yuan, Xing Xie, and Shiqiang Yang. Little is much: Bridging cross-platform behaviors through overlapped crowds. In *Proceedings of the AAAI Conference on Artificial Intelligence*, volume 30, 2016.

Xiaoyong Jin, Youngsuk Park, Danielle Maddix, Hao Wang, and Yuyang Wang. Domain adaptation for time series forecasting via attention sharing. In *International Conference on Machine Learning*, pp. 10280–10297. PMLR, 2022.

Muhammad Murad Khan, Roliana Ibrahim, and Imran Ghani. Cross domain recommender systems: A systematic literature review. *ACM Computing Surveys (CSUR)*, 50(3):1–34, 2017.

Ananya Kumar, Tengyu Ma, and Percy Liang. Understanding self-training for gradual domain adaptation. In *International Conference on Machine Learning*, pp. 5468–5479. PMLR, 2020.

Seiichi Kuroki, Nontawat Charoenphakdee, Han Bao, Junya Honda, Issei Sato, and Masashi Sugiyama. Unsupervised domain adaptation based on source-guided discrepancy. In *AAAI*, pp. 4122–4129, 2019.

Pan Li and Alexander Tuzhilin. Dual metric learning for effective and efficient cross-domain recommendations. *IEEE Transactions on Knowledge and Data Engineering*, 35(1):321–334, 2021.

Tianyi Liu, Zihao Xu, Hao He, Guang-Yuan Hao, Guang-He Lee, and Hao Wang. Taxonomy-structured domain adaptation. In *International Conference on Machine Learning*, pp. 22215–22232. PMLR, 2023.

Mingsheng Long, Zhangjie Cao, Jianmin Wang, and Michael I. Jordan. Conditional adversarial domain adaptation. In *NIPS*, pp. 1647–1657, 2018.

Kezhi Lu, Qian Zhang, Danny Hughes, Guangquan Zhang, and Jie Lu. Amt-cdr: A deep adversarial multi-channel transfer network for cross-domain recommendation. *ACM Transactions on Intelligent Systems and Technology*, 2024.

Tong Man, Huawei Shen, Xiaolong Jin, and Xueqi Cheng. Cross-domain recommendation: An embedding and mapping approach. In *IJCAI*, volume 17, pp. 2464–2470, 2017.

Massimiliano Mancini, Samuel Rota Bulo, Barbara Caputo, and Elisa Ricci. Adagraph: Unifying predictive and continuous domain adaptation through graphs. In *CVPR*, pp. 6568–6577, 2019.

Andriy Mnih and Russ R Salakhutdinov. Probabilistic matrix factorization. *Advances in neural information processing systems*, 20, 2007.

Ravi Nahta, Ganpat Singh Chauhan, Yogesh Kumar Meena, and Dinesh Gopalani. Cf-mgan: Collaborative filtering with metadata-aware generative adversarial networks for top-n recommendation. *Information Sciences*, 689:121337, 2025.

Le Thanh Nguyen-Meidine, Atif Belal, Madhu Kiran, Jose Dolz, Louis-Antoine Blais-Morin, and Eric Granger. Unsupervised multi-target domain adaptation through knowledge distillation. In *Proceedings of the IEEE/CVF Winter Conference on Applications of Computer Vision*, pp. 1339–1347, 2021.

Sinno Jialin Pan and Qiang Yang. A survey on transfer learning. *TKDE*, 22(10):1345–1359, 2009.

Sinno Jialin Pan, Ivor W Tsang, James T Kwok, and Qiang Yang. Domain adaptation via transfer component analysis. *TNN*, 22(2):199–210, 2010.

Xingchao Peng, Qinxun Bai, Xide Xia, Zijun Huang, Kate Saenko, and Bo Wang. Moment matching for multi-source domain adaptation. In *Proceedings of the IEEE/CVF International Conference on Computer Vision*, pp. 1406–1415, 2019.

Dilruk Perera and Roger Zimmermann. Exploring the use of time-dependent cross-network information for personalized recommendations. In *Proceedings of the 25th ACM international conference on Multimedia*, pp. 1780–1788, 2017.

Viraj Prabhu, Shivam Khare, Deeksha Kartik, and Judy Hoffman. Sentry: Selective entropy optimization via committee consistency for unsupervised domain adaptation. In *Proceedings of the IEEE/CVF International Conference on Computer Vision*, pp. 8558–8567, 2021.

Dimitrios Rafailidis and Fabio Crestani. A collaborative ranking model for cross-domain recommendations. In *Proceedings of the 2017 ACM on Conference on Information and Knowledge Management*, pp. 2263–2266, 2017.

Nils Reimers and Iryna Gurevych. Making monolingual sentence embeddings multilingual using knowledge distillation. In *Proceedings of the 2020 Conference on Empirical Methods in Natural Language Processing*. Association for Computational Linguistics, 11 2020. URL `https://arxiv.org/abs/2004.09813`.

Kuniaki Saito, Kohei Watanabe, Yoshitaka Ushiku, and Tatsuya Harada. Maximum classifier discrepancy for unsupervised domain adaptation. In *CVPR*, pp. 3723–3732, 2018.

Swami Sankaranarayanan, Yogesh Balaji, Carlos D. Castillo, and Rama Chellappa. Generate to adapt: Aligning domains using generative adversarial networks. In *CVPR*, pp. 8503–8512, 2018.

Onur Tasar, Yuliya Tarabalka, Alain Giros, Pierre Alliez, and Sébastien Clerc. Standardgan: Multi-source domain adaptation for semantic segmentation of very high resolution satellite images by data standardization. In *Proceedings of the IEEE/CVF Conference on Computer Vision and Pattern Recognition Workshops*, pp. 192–193, 2020.

Eric Tzeng, Judy Hoffman, Kate Saenko, and Trevor Darrell. Adversarial discriminative domain adaptation. In *CVPR*, pp. 7167–7176, 2017.

Hao Wang, Naiyan Wang, and Dit-Yan Yeung. Collaborative deep learning for recommender systems. In *KDD*, pp. 1235–1244, 2015.

Hao Wang, Hao He, and Dina Katabi. Continuously indexed domain adaptation. In *ICML*, 2020a.

Wenhui Wang, Furu Wei, Li Dong, Hangbo Bao, Nan Yang, and Ming Zhou. Minilm: Deep self-attention distillation for task-agnostic compression of pre-trained transformers. *Advances in Neural Information Processing Systems*, 33:5776–5788, 2020b.

Xinghua Wang, Zhaohui Peng, Senzhang Wang, Philip S Yu, Wenjing Fu, and Xiaoguang Hong. Cross-domain recommendation for cold-start users via neighborhood based feature mapping. In *Database Systems for Advanced Applications: 23rd International Conference, DASFAA 2018, Gold Coast, QLD, Australia, May 21-24, 2018, Proceedings, Part I 23*, pp. 158–165. Springer, 2018.

Zihao Xu, Hao He, Guang-He Lee, Yuyang Wang, and Hao Wang. Graph-relational domain adaptation. In *ICLR*, 2022.

Zihao Xu, Guang-Yuan Hao, Hao He, and Hao Wang. Domain-indexing variational bayes: Interpretable domain index for domain adaptation. In *ICLR*, 2023.

Chunfeng Yang, Huan Yan, Donghan Yu, Yong Li, and Dah Ming Chiu. Multi-site user behavior modeling and its application in video recommendation. In *Proceedings of the 40th International ACM SIGIR Conference on Research and Development in Information Retrieval*, pp. 175–184, 2017.

Tianzi Zang, Yanmin Zhu, Haobing Liu, Ruohan Zhang, and Jiadi Yu. A survey on cross-domain recommendation: taxonomies, methods, and future directions. *ACM Transactions on Information Systems*, 41 (2):1–39, 2022.

Qian Zhang, Jie Lu, Dianshuang Wu, and Guangquan Zhang. A cross-domain recommender system with kernel-induced knowledge transfer for overlapping entities. *IEEE transactions on neural networks and learning systems*, 30(7):1998–2012, 2018.

Qian Zhang, Peng Hao, Jie Lu, and Guangquan Zhang. Cross-domain recommendation with semantic correlation in tagging systems. In *2019 International Joint Conference on Neural Networks (IJCNN)*, pp. 1–8. IEEE, 2019a.

Yuchen Zhang, Tianle Liu, Mingsheng Long, and Michael I Jordan. Bridging theory and algorithm for domain adaptation. *arXiv preprint arXiv:1904.05801*, 2019b.

Feng Zhu, Chaochao Chen, Yan Wang, Guanfeng Liu, and Xiaolin Zheng. Dtcdr: A framework for dual-target cross-domain recommendation. In *Proceedings of the 28th ACM international conference on information and knowledge management*, pp. 1533–1542, 2019.

Feng Zhu, Yan Wang, Chaochao Chen, Guanfeng Liu, and Xiaolin Zheng. A graphical and attentional framework for dual-target cross-domain recommendation. In *IJCAI*, volume 21, pp. 39, 2020.

Feng Zhu, Yan Wang, Chaochao Chen, Jun Zhou, Longfei Li, and Guanfeng Liu. Cross-domain recommendation: challenges, progress, and prospects. *arXiv preprint arXiv:2103.01696*, 2021a.

Feng Zhu, Yan Wang, Jun Zhou, Chaochao Chen, Longfei Li, and Guanfeng Liu. A unified framework for cross-domain and cross-system recommendations. *IEEE Transactions on Knowledge and Data Engineering*, 2021b.

Yaochen Zhu and Zhenzhong Chen. Mutually-regularized dual collaborative variational auto-encoder for recommendation systems. In *Proceedings of The ACM Web Conference 2022*, pp. 2379–2387, 2022.

Yang Zou, Zhiding Yu, B.V.K. Vijaya Kumar, and Jinsong Wang. Unsupervised domain adaptation for semantic segmentation via class-balanced self-training. In *Proceedings of the European Conference on Computer Vision (ECCV)*, September 2018.